# A First-Principles Study of L-Shell Iron and Chromium Opacity at Stellar Interior Temperatures

V. V. Karasiev,[1] S. X. Hu,[1] N. R. Shaffer,[1] and G. Miloshevsky[2]

[1]Laboratory for Laser Energetics, University of Rochester
[2]Department of Mechanical and Nuclear Engineering, Virginia Commonwealth University

Accurate prediction of optical properties of matter across a wide range of material densities and temperatures is of great importance in planetary science, astrophysics, and inertial confinement fusion.[1–4] Building a reliable opacity model for materials under extreme conditions is one of the grand challenges in high-energy-density physics, especially across the most complicated warm-dense-matter (WDM) domain of thermodynamic conditions when both the coulomb coupling parameter and the electron degeneracy are close to unity. The traditional opacity models based on physics of isolated atoms when the important plasma density and temperature effects such as Stark broadening, ionization potential depression (IPD), and continuum lowering are incorporated via corrections often become unreliable beyond the ideal plasma conditions.

In this work we use a first-principles density functional theory (DFT)-based methodology to calculate optical properties (mass-absorption coefficient and opacity) of Cr and Fe at stellar interior temperatures corresponding to recent experiments.[5,6] The purpose is to explore whether or not such *ab initio* calculations can resolve the reported disagreement between previous atomic physics calculations and measured data.[5,6] Our DFT results are compared to the real-space Green's function (RSGF) method[7–9] and to the radiative emissivity and opacity of dense plasmas (REODP) atomistic model.[10]

A free-energy DFT-based methodology for optical property calculations in the WDM domain presented in Ref. 11 handles deeply bounded core electrons on an equal footing with free electrons in the system and self-consistently takes into account effects such as quasistatic pressure broadening due to interaction with neighboring ions [in case of calculations on molecular dynamics (MD) multi-ion supercell snapshots], the IPD, continuum lowering, and Fermi surface rising. The methodology incorporates a combination of the Kubo–Greenwood (KG) optical data, evaluated on a set of the *ab initio* molecular dynamics (AIMD) snapshots, with a periodic single-atom-in-a-cell calculation at the same thermodynamic conditions. KG calculations on snapshots account for the influence of the local plasma environment, which is important for photon energies near the L and K edges. Kubo–Greenwood data from periodic calculations with single atom cover the tail regions beyond the L and K edges.

The Kubo–Greenwood formulation implemented in the post-processing code *KGEC* (Kubo–Greenwood electronic conductivity) for use with the *Quantum-Espresso* large-scale DFT-based simulation package, *KGEC@Quantum-Espresso*,[12,13] calculates the frequency-dependent real and imaginary parts of electric conductivity, $\sigma_1(\omega)$ and $\sigma_2(\omega)$; the real part of the index of refraction, $n(\omega)$; the absorption coefficient, $\alpha(\omega) = \sigma_1(\omega)\,[4\pi/n(\omega)c]$; and the mass-absorption coefficient $\alpha m(\omega) = \alpha(\omega)/\rho$ (where $c$ is the speed of light, $\rho$ is the material density, and the photon energy is $\hbar\omega = h\nu$). The optical properties were calculated for a single-atom-in-a-cell and as an average over a selected set of uncorrelated two-atom MD snapshots. Eventually the grouped Rosseland mean opacities for a narrow 4-eV group of photon energies are calculated.

In this study we are focused on the L-shell absorption and opacity calculations at temperatures when the deep 1*s* bands remain fully populated. Therefore, 1*s* frozen-core projector augmented wave (PAW) data sets for Fe and Cr are generated using the *ATOMPAW* code.[14] A small augmentation sphere radius $r_{\mathrm{PAW}} = 0.35$ bohr requires a relatively high cutoff energy of $E_{\mathrm{cut}} = 800$ Ry to converge electronic pressure. The optical properties are calculated using the Kubo–Greenwood formulation implemented within

the PAW formalism in *KGEC@Quantum-Espresso*[12,13,15] packages. The Gaussian broadening was done with relatively large $\delta$ = 15 eV due to the sparsity of states in the case of the single-atom-in-a-cell calculations.

Table I shows free-electron densities of chromium and iron calculated at $T$ = 182 eV and $\rho$ = 0.161 g/cm$^3$ and 0.165 g/cm$^3$, respectively. Theoretical predictions by all three methods are in very good agreement; relative differences of the REODP and RSGF values with respect to the DFT data do not exceed 2% and 4%, respectively, matching the experimental value of 3 × 10$^{22}$ cm$^{-3}$ from measurements for Cr and Fe.

Table I: Free-electron density (in cm$^{-3}$ units) for chromium and iron at $T$ = 182 eV and $\rho_{Cr}$ = 0.161 g/cm$^3$, $\rho_{Fe}$ = 0.165, respectively, as predicted by the DFT, REODP, and RSGF methods.

| System | DFT | REODPe | RSGF |
|---|---|---|---|
| Cr | 3.00 × 10$^{22}$ | 2.95 × 10$^{22}$ | 3.12 × 10$^{22}$ |
| Fe | 3.00 × 10$^{22}$ | 2.95 × 10$^{22}$ | 3.12 × 10$^{22}$ |

Figure 1 shows our main results for opacity of chromium and iron calculated at $T$ = 182 eV and material density of 0.161 g/cm$^3$ and 0.165 g/cm$^3$, respectively, alongside with experimental measurements. At short wavelengths below ~9.5 A [the L-shell bound-continuum region for photon energies above ~1.2 keV], the agreement between all three theoretical data and experiments is very good for chromium: the REODP curve goes straight through the experimental data, while the DFT and RSGF data are located slightly below, touching the yellow-shaded experimental error bars. The situation for iron is different; opacity predicted by theoretical methods in the L-shell bound-continuum region is underestimated by about 50% as compared to the experimental data. The REODP curve is slightly closer to the experimental data as compared to the DFT single-atom-in-a-cell and RSGF simulations.

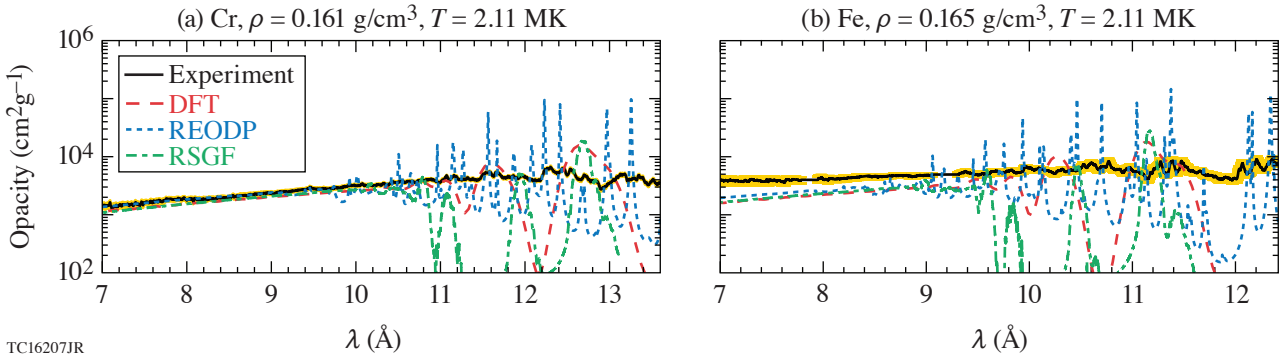


Figure 1
Opacity of iron and chromium at 0.165 g/cm$^3$ and 0.165 g/cm$^3$, respectively. A comparison is made between the experimental measurements (solid black curve, the yellow-shaded area corresponds to the experimental measurements error) and three theoretical predictions at $T$ = 182 eV.

In the wavelength range above 9.5 A, opacity is dominated mostly by the bound–bound absorption lines. The DFT and RSGF calculations predict a small set of smooth and strong discrete lines separated by deep windows. The REODP method predicts a richer spectrum of sharp peaks. The REODP-calculated opacities represent the detailed all-line spectra without any kind of averaging into spectral groups. The peaks and wings of the lines are resolved with a high accuracy. The spectral lines are roughly centered on the experimental opacity curves. However, none of our theoretical predictions is close to the measured bound–bound opacity in that range. The DFT predictions for the bound–bound absorption can be improved by performing the Kubo–Greenwood optical calculations on top of the AIMD snapshots for larger supercells including more than two atoms by considering more-realistic charge-state distributions. However, such demanded calculations, on both memory and time, are currently out of reach.

This material is based upon work supported by the Department of Energy National Nuclear Security Administration under Award Number DE-NA0003856, U.S. National Science Foundation PHY Grants No. 1802964 and No. 2205521, Defense Threat

Reduction Agency under Grants No. HDTRA1-19-1-0019 and HDTRA1-20-2-0001, the University of Rochester, and the New York State Energy Research and Development Authority. This research used resources of the National Energy Research Scientific Computing Center, a DOE Office of Science User Facility supported by the Office of Science of the U.S. Department of Energy under Contract No. DE-AC02-05CH11231 using NERSC award FES-ERCAP0021234.

1. J. J. Fortney and N. Nettelmann, Space Sci. Rev. **152**, 423 (2010).
2. C. A. Iglesias, F. J. Rogers, and D. Saumon, Astrophys. J. Lett. **569**, L111 (2002).
3. S. X. Hu *et al.*, Phys. Rev. E **90**, 033111 (2014).
4. S. X. Hu *et al.*, Phys. Plasmas **22**, 056304 (2015).
5. J. E. Bailey *et al.*, Nature **517**, 56 (2015).
6. T. Nagayama *et al.*, Phys. Rev. Lett. **122**, 235001 (2019).
7. J. J. Rehr and R. C. Albers, Rev. Mod. Phys. **72**, 621 (2000).
8. Y. Wang *et al.*, Phys. Rev. Lett. **75**, 2867 (1995).
9. N. Shaffer and C. E. Starrett, Phys. Rev. E **150**, 015203 (2022).
10. G. Miloshevsky and A. Hassanein, Phys. Rev. E **92**, 033109 (2015).
11. V. V Karasiev and S. X. Hu, Phys. Rev. E **103**, 033202 (2021).
12. L. Calderín, V. V. Karasiev, and S. B. Trickey, Comput. Phys. Commun. **221**, 118 (2017).
13. P. Giannozzi *et al.*, J. Phys.: Condens. Matter **21**, 395502 (2009).
14. N. A. W. Holzwarth, A. R. Tackett, and G. E. Matthews, Comp. Phys. Commun. **135**, 329 (2001).
15. V. V. Karasiev, T. Sjostrom, and S. B. Trickey, Comput. Phys. Commun. **185**, 3240 (2014).